

Field Validation of Algebraic Equations for Stack and Wind Driven Air Infiltration Calculations

I.S. Walker, Ph.D.

Member ASHRAE

D.J. Wilson, Ph.D., P.E.

Member ASHRAE

Explicit algebraic equations for calculation of wind and stack driven ventilation were developed by parametrically matching exact solutions to the flow equations for building envelopes. These separate wind and stack effect flow calculation procedures were incorporated in a simple natural ventilation model, AIM-2, with empirical functions for superposing wind and stack effect, and for estimating wind shelter. There were three major improvements over previous simplified ventilation calculations: a power law pressure-flow relationship is used to develop the flow equations from first principles, the furnace or fireplace flue is included as a separate leakage site, and the model differentiates between houses with basements, slab-on-grade, and crawlspaces. Over 3400 hours of measured ventilation rates from the test houses at the Alberta Home Heating Research Facility were used to validate the predictions of ventilation rates and to compare the AIM-2 predictions to those of other ventilation models. The AIM-2 model had bias and scatter errors of less than 15% for wind-dominated ventilation, and less than 7% for buoyancy (stack-effect) dominated cases.

INTRODUCTION

This paper derives the technical basis for the relationships used in the AIM-2 air infiltration model, and to describe the validation procedure used to evaluate its predictive skill. Some of the algebraic equations used in AIM-2 were presented in Walker and Wilson (1990a). A simplified version of AIM-2 has also been used for calculating attic ventilation rates by Walker et al. (1995). However, no derivation or physical explanation of the relationships was given.

AIM-2 combines ideas from previous ventilation models, particularly the LBL model of Sherman and Grimsrud (1980) with new concepts originally developed by Walker (1989) that account for power law envelope leakage, separate flue/fireplace leaks and the differences between houses with basements, slab-on-grade, and crawlspaces. Also added are additional refinements regarding wind shelter calculations, and adjusting wind speeds from the measurement site to the building.

Although AIM-2 has not been published in complete form, the algorithms have been used since they were listed by Walker and Wilson (1990a). AIM-2 is used in the HOT2000/AUDIT2000 series of energy analysis programs produced by Natural Resources Canada (CHBA 1994). AIM-2 has been used by other researchers in studies to model infiltration rates in residential buildings. The predictions of AIM-2 were evaluated by comparisons with measured data by Palmiter and Bond (1994) and Palmiter et al. (1991), and by developing a simple method for combining natural and mechanical ventilation by Palmiter and Bond (1991). In another study by Hamlin and Pushka (1994), the AIM-2 algorithms were used to predict infiltration rates for an indoor air quality model.

Iain S. Walker is staff scientist, Lawrence Berkeley National Laboratory, Berkeley, CA and David Wilson is a professor in the Department of Mechanical Engineering, University of Alberta, Edmonton, Canada.

In the present study, over 3400 hours of measured ventilation rates in two houses were used to test AIM-2. This is part of the data base of ventilation measurements from six houses of the Alberta Home Heating Research Facility that includes houses with other magnitudes and distributions of leakage. The large set of measured data provided a wide range of weather conditions and house leakage distributions, in order to exercise all parts of the model. Large quantities of measured data were required for validation because of the substantial hourly variation of natural ventilation rates.

The measured data were not used to tune coefficients in the AIM-2 model equations. Instead, the measurements were used to determine typical errors that might occur in calculating ventilation rates based on parameters that are easily determined for most houses. That is, rather than specifying the size and location of every leak (which is not possible in most practical situations) the parameters used in the model are the envelope leakage characteristics [usually determined using a fan pressurization test, e.g., ASTM (1995) or CGSB (1986)] and simple estimates of the envelope leakage distribution. The evaluation also included comparison of the measurements with other simple ventilation models. The other models included for comparison are: the LBL (USA) model (Sherman and Grimsrud 1980), the VFE (Canada), the variable n extensions of the LBL model by Yuill (1985) and by Reardon (1989), the NRC (Canada) model of Shaw (1985), and the BRE (U.K.) model of Warren and Webb (1980).

MODEL DEVELOPMENT

The development of the AIM-2 model began with deriving an exact numerical solution to the non-linear combined wind pressure and buoyancy-driven mass flow balance into and out of the building. This exact solution is presented in the Appendix. The algebraic relationships used in AIM-2 were then developed by trial and error as closed form approximations to this exact solution.

For AIM-2, wind and stack effect flows were determined separately, then superposed as a sum of effective pressures, with a correction term that accounts for the interaction of wind and stack induced pressure. This wind and stack effect interaction term is the only empirical constant determined by comparing the AIM-2 equations to measured data.

The AIM-2 model improves estimates of air infiltration rates by incorporating a power law pressure-flow relationship, $Q = C\Delta P^n$, into the model from first principles. This is done by treating the furnace or fireplace flue as a separate leakage site with its own wind shelter, and by locating the flue outlet above the house (depending on the actual flue height), rather than grouping the flue leakage with the other building leaks, as in other models.

The following simplifying assumptions were used in the development of the exact ventilation calculations. The building was a single, well mixed zone; wall leaks were evenly distributed over four walls, evenly distributed with height, the flue was filled with air at indoor room temperature, and the flow through all building leaks was characterized by the same power law exponent of pressure n .

In order to simplify the calculation of wind factor, the following assumptions were made about the pressure coefficients in crawl spaces and attics. Firstly, the pressure coefficient on the exterior floor of the building in a crawl space can be approximated by averaging the pressure coefficients on the four external surfaces of the crawl space. Secondly, the pressures on crawl space surfaces were the same as on the walls above them on each side of the building. Also, the pressure coefficient for the ceiling (i.e. for the attic) was assumed to be the average of the exposed attic roof and soffit surfaces.

Determining Algebraic Approximations to Exact Numerical Solutions

A key part of AIM-2 was the development of the algebraic approximations to the exact numerical solutions of the flow equations. Algebraic functions were chosen by looking at plots

of the wind and stack factors' (f_s and f_w) dependence on the leakage location and pressure exponent parameters. A list of candidate algebraic functions that had the same shape and asymptotic limits was then made. The algebraic functions for each parameter were then chosen sequentially, with the most significant parameters selected first. Less significant parameters were then combined in such a way that they did not modify the existing functions. The functions for the most significant parameters were chosen to capture most of the variability (e.g., the dependence on wall leakage). The addition or multiplication of other functions were for secondary effects (e.g., the separate furnace flue leakage). Thus a composite function was built up with several primary functions embedded within it. The algebraic equations in this model were developed based on several guiding principals:

- The functions had to retain dimensional consistency.
- The functions had to be as simple as possible (e.g., no hyperbolic tangents) so that they could be used in engineering design (spreadsheet) calculations.
- The functions had to be robust (i.e. that could tolerate any possible input parameter, e.g., limits of impermeable walls combined with leaky ceilings) and smooth, so as not to give unusual values for specific cases.
- The constants and exponents were chosen to be integers, proper fractions or the leakage parameters themselves.

Power Law Flow Relationship

The authors and others, including Beach (1979), Sulatisky (1984), and Warren and Webb (1980) performed fan pressurization tests of houses. These tests, as well as theoretical considerations from Walker et al. (1996), showed that the orifice flow assumption used in the many infiltration models is unrealistic, and that it is better to use a power law pressure-flow relationship:

$$Q = C\Delta P^n \quad (1)$$

The parameters C and n are usually found from fan pressurization tests of the building. For a typical residential building $n \sim 0.67$, about midway in its range from $n = 0.50$ for orifice flow to $n = 1.0$ for fully developed laminar flow.

Leakage Distribution

Pioneering work by Sherman and Grimsrud (1980) introduced the idea of using a set of quantitative parameters to describe the leakage distribution of a building envelope, and to determine the independent stack-driven and wind-driven flow rates in terms of stack and wind factors, f_s and f_w . Sherman and Grimsrud characterized the leakage distribution in terms of R , the fraction of the 4 Pa fan pressurization leakage area (A_4) in the floor plus the ceiling, and X , the difference in leakage between the floor and ceiling as fractions of the total leakage. They defined the "floor" leakage as those leakage sites that are located at (or near) the level of the building floor that rests on the basement walls, slab-on-grade, or crawlspace. The "ceiling" leakage includes the leakage sites that are at (or near) the ceiling level of the upper floor of the building.

In AIM-2, the furnace/fireplace flue is treated separately from the other leaks, and additional parameters are introduced to account for this separate leak: the flue leakage fraction Y and a flue height parameter Z_f . The leakage distribution is specified in terms of the ratio parameters R , X , and Y , that are calculated from the leakage coefficients C_{flue} , C_c , C_f , and C_w , in Equation (1) rather than from the A_4 leakage areas.

Explicit solutions require the assumption that the exponent n in Equation (1) is the same for all leakage sites. In this case, the total leakage coefficient C is simply the algebraic sum

$$C = C_c + C_f + C_w + C_{flue} \quad (2)$$

Leakage distribution parameters are defined using the format suggested by Sherman (1980), but using C instead of leakage area A_d , and with the addition of a separate flue fraction Y .

$$R = \frac{C_c + C_f}{C} \quad \text{ceiling - floor sum} \quad (3)$$

$$X = \frac{C_c - C_f}{C} \quad \text{ceiling - floor difference} \quad (4)$$

$$Y = \frac{C_{flue}}{C} \quad \text{flue fraction} \quad (5)$$

In addition to the distributed leakage of the building envelope expressed in terms of R , X , and Y , the normalized height Z_f of the flue is given by

$$Z_f = \frac{H_f}{H} \quad (6)$$

Stack Effect Infiltration

The flow induced by stack effect Q_s is given by

$$Q_s = C f_s \Delta P_s^n \quad (7)$$

where ΔP_s is the driving pressure for buoyancy-driven stack-effect flow.

$$\Delta P_s = \rho_{out} g H \frac{|T_{in} - T_{out}|}{T_{in}} \quad (8)$$

The stack factor f_s was determined using the numerical solution of the exact flow equations to calculate the stack driven ventilation rate flowrate Q_s in Equation (7) over a wide range of R , X , Y , Z_f , and flow exponent n . The algebraic approximation for stack factor was developed (as discussed earlier) to give the same general dependence of f_s on these parameters as the numerical solution of the nonlinear flow balance equations. The resulting approximation for f_s is given by Equation (9). The functional form of this approximation was selected to produce the correct limits for f_s when all leakage is concentrated in the walls ($R = 0$), or in the floor and ceiling ($R = 1$), for the ceiling-floor difference ratio limits of $X = +1.0$, -1.0 , and at the $X = 0$ midpoint.

$$f_s = \left(\frac{1 + nR}{n + 1} \right) \left(\frac{1}{2} - \frac{1}{2} M^{5/4} \right)^{n+1} + F \quad (9)$$

where

$$M = \frac{[X + (2n + 1)Y]^2}{2 - R} \quad \text{for} \quad \frac{[X + (2n + 1)Y]^2}{2 - R} \leq 1 \quad (10)$$

with a limiting value of

$$M = 1.0 \text{ for } \frac{[X + (2n + 1)Y]^2}{2 - R} > 1 \quad (11)$$

The additive flue function F is given by

$$F = nY(Z_f - 1)^{\frac{3n-1}{3}} \left(1 - \frac{3(X_c - X)^2 R^{1-n}}{2(Z_f + 1)} \right) \quad (12)$$

where

$$X_c = R + \frac{2(1 - R - Y)}{n + 1} - 2Y(Z_f - 1)^n \quad (13)$$

The flue factor F in Equation (9) is always additive because the flue outlet is the highest leakage site and will always act to increase the ventilation flows.

With very strong flue exfiltration, even the ceiling can become an infiltration site, through which attic air is drawn into the building. The variable X_c is the critical value of the ceiling-floor leakage difference X at which the neutral level (zero indoor to outdoor pressure difference) is located at the ceiling in the exact numerical solution. For $X > X_c$ the neutral level will be above the ceiling, and air will flow in through the ceiling. For $X < X_c$ room air will exfiltrate through the ceiling. (These flow directions assume $T_{in} > T_{out}$, and will be reversed if $T_{out} > T_{in}$.) The role of the flue in reducing ceiling exfiltration is evident from the contribution of the Y factor in Equation (13).

The stack factor f_s from Equation (9) is shown in Figure 1 for typical values of $n = 0.67$, $Z_f = 1.5$, and $Y = 0.2$, and for no flue, $Y = 0$. Figure 1 shows that treating the flue as a separate leakage site with a stack height above the ceiling has a significant effect on the stack factor f_s . In addition, Figure 1 shows the reduction in f_s as leakage becomes concentrated at single locations, i.e. when $X = R$. When $R = 0$ then $X = 0$ and only a single point can be determined. In Figure 1, the value of f_s for $R = 0$ is given by a cross for the no flue case and by a star for $Y = 0.2$.

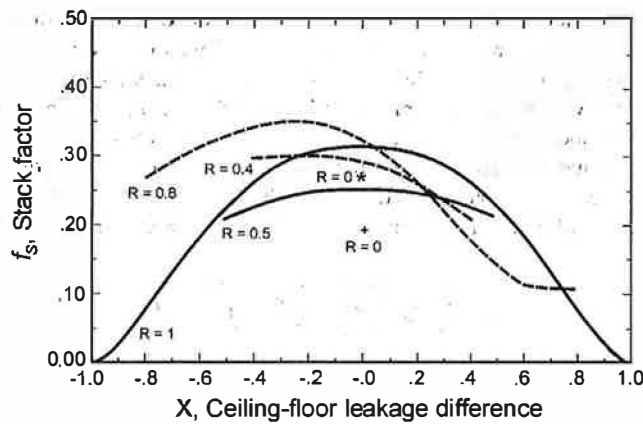


Figure 1. AIM-2 [Equation (9)] stack factor f_s with no flue leakage ($Y = 0$) (solid line) and 20% of leakage in flue ($Y = 0.2$), and $Z_f = 1.5$ (dashed line)

Because the AIM-2 relationships for calculating f_s are approximations, they do not match the exact numerical solution perfectly. Differences between the stack factor estimated by Equation (9) and the exact numerical solution are about ± 0.005 for a house with $Y = 0$ (no flue) to ± 0.01 for $Y = 0.2$. With f_s typically about 0.3, these differences represent errors of about $\pm 1.5\%$ in f_s . The maximum difference between exact and approximate stack factors can be as high as 0.03, about 10% in f_s and in Q_s .

Wind Effect Infiltration

For AIM-2 we proposed two different models, one for houses with basements or slab on grade construction, and another for houses with crawl spaces. The difference between the two models is the way the pressure coefficient is applied to the floor level leaks. For basement or slab on grade construction, the floor level leaks are split into four equal parts below each wall, each assumed to have the same pressure coefficient as the walls above them. For crawlspaces, the pressure coefficients on the four walls are averaged and used as the pressure coefficient in the crawlspace acting on the floor level leakage between the house and the crawlspace. For both cases the wind pressure coefficients measured by Akins et al. (1979) wind tunnel simulations were used for the walls of the building.

The attic pressure coefficient in AIM-2 was assumed to be an eave-length weighted average of the pressure coefficients on the eave and end wall vents, and the roof surface vents. The eave vents were assumed to have the same pressure as the adjacent wall. The attic roof vents were assumed to have a size equal to the sum of the eave vents.

These algebraically averaged wind pressure coefficients imply a linear relationship between pressure and flow, which is clearly not true if $n \neq 1$ in Equation (1). The errors caused by algebraically averaging pressure coefficients were determined by applying the exact non-linear flow balancing equations to find the actual pressure coefficients on the floor and ceiling required to balance the flow in and out of attics or crawlspaces. The algebraic average pressure coefficient for the four walls of a square building with the wind normal to the upwind wall (the most extreme case) was -0.25 , using pressure coefficients from Akins et al. (1979). The exact equations showed that the actual pressure coefficient required to balance the flows was -0.3 , with $n = 0.67$. This result showed that a simple algebraic average of wall pressure coefficients was sufficiently accurate to define crawl space or attic pressures.

Wind Shelter Effect on Wind Pressures

The wind induced infiltration rate Q_w is given by

$$Q_w = C f_w \Delta P_w^n \tag{14}$$

where ΔP_w is given by

$$\Delta P_w = \frac{P_{out} (S_w U)^2}{2} \tag{15}$$

Local shielding by nearby buildings, trees and obstructions is difficult to estimate by inspecting the building site, and uncertainty in estimating the local shelter coefficient S_w is often the major source of error in estimating wind driven infiltration flow rates. Previous ventilation studies have included shelter only in broad classes, with sharp changes from class to class. For example, Sherman and Grimsrud (1980) used a look-up table with five descriptive classes of shelter such as "Light local shielding with few obstructions".

To allow for changes in wind shelter with wind direction, AIM-2 uses the shelter interpolation function suggested by Walker and Wilson (1991) to determine the shelter for the building S_{wo} . This function takes estimates of wind shelter for winds perpendicular to each side of the building and calculates wind shelter for any intermediate angle. S_{wo} is combined in AIM-2 with a different coefficient (S_{wflue}) for the top of the flue stack to give an improved estimate of the total shielding. These wind shelter factors are combined linearly:

$$S_w = S_{wo}(1 - Y) + S_{wflue}(1.5Y) \tag{16}$$

where the factor 1.5 is an empirical adjustment found by comparing the AIM-2 model predictions to the exact numerical solution where each leakage site has its own pressure coefficient and shelter. $S_{wflue} = 1.0$ for an unsheltered flue, which protrudes above surrounding obstacles, and $S_{wflue} = S_{wo}$ for a flue top that has the same wind shelter as the building walls. With no flue, $Y = 0$ and $S_w = S_{wo}$.

Table 1 gives the AIM-2 wind shelter factor estimates for winds perpendicular to the sides of the building. This table uses the same shielding class description suggested by Sherman and Grimsrud (1980), with the addition of a new class of "complete shielding". However, it is important to note that although the terrain classes are the same, the shelter values in Table 1 are not the same as Sherman and Grimsrud's "generalized shielding coefficient".

Table 1. Estimates of Shelter Coefficient

Shelter Coefficient, S_w	Description
1.00	No obstructions or local shielding
0.90	Light local shielding with few obstructions within two building heights
0.70	Local shielding with many large obstructions within two building heights
0.50	Heavily shielded, many large obstructions within one building height
0.30	Complete shielding with large buildings immediately adjacent

Adjusting Windspeed for Local Terrain

The pressure coefficients used to find f_w were taken from wind tunnel tests. For most wind tunnel tests the wind pressure coefficient C_p was calculated using a reference wind speed at eaves height H . Most meteorological data is measured at greater heights and must be converted to the eave height to account for the change in windspeed with height in the atmospheric boundary layer. Walker and Wilson (1990b) showed how meteorological windspeeds measured remotely from the building site can be converted to an eaves height windspeed at the building, assuming a power law boundary layer wind velocity profile. Wieringa (1980) recommended using the wind speed at the top of the constant shear stress surface layer when converting wind speeds from one location to another. Wieringa estimated this height to be about 80 m plus the area-averaged height δ_z of the roughness elements between the two locations.

Using this reference height, the relationship for converting airport windspeeds to local conditions is

$$U = \left(\frac{80 + \delta_z}{H_{met}} \right)^{p_{met}} \left(\frac{H_{ref}}{80 + \delta_z} \right)^p U_{met} \tag{17}$$

p and p_{met} depend on windspeed, ground roughness, solar insolation, and atmospheric stability. Irwin (1979) gave values of p from 0.12 to 0.47 for a wide range of conditions. For typical urban housing he proposed using $p \sim 0.3$, and for meteorological stations located at airports or other exposed sites $p \sim 0.15$.

Houses with Basements or Slab-on-Grade Construction

The wind factor f_w was found by using the exact flow balance equations to determine Q_w numerically. f_w was then determined by rearranging Equation (14) and substituting this value of Q_w and the appropriate value of ΔP_w . The approximating function for f_w was generated using the methods discussed earlier, by calculating f_w over a wide range of leakage parameters and finding functional forms that would reproduce the same characteristic dependence on the leakage location and pressure exponent.

The exact numerical solution for f_w , and its approximating function depend on the set of wind pressure coefficients used. In AIM-2, the wind pressure coefficients from Akins et al. (1979) and the flue cap pressure coefficient from Haysom and Swinton (1987) were used. Using these pressure coefficients, f_w was found to be approximated by

$$f_w = 0.19(2-n) \left[1 - \left(\frac{X+R}{2} \right)^{\left(\frac{3}{2} - Y \right)} \right] - \frac{Y}{4}(J - 2YJ^4) \quad (18)$$

where

$$J = \frac{X+R+2Y}{2} \quad (19)$$

The functional form for f_w was chosen to produce the correct behavior for the limiting values of all leakage concentrated in either walls, floor or ceiling, and for $X = 0$ where the floor and ceiling leakage are equal. The flue height Z_f does not appear in Equation (18) because flue height is only felt very weakly through the change in windspeed at the flue/fireplace outlet.

The wind factor calculated using Equation (18) is shown in Figure 2 for $n = 2/3$, $Y = 0.2$, and for no flue ($Y = 0$). This figure shows that there is little effect on wind factor f_w when the flue leakage is considered as a hole in the ceiling venting into the attic (equivalent to $Y = 0$) or as a separate leakage site with its own flue cap pressure coefficient above the roof ($Y = 0.2$). In the same way as for the stack factor, when $R = 0$ then $X = 0$ and only a single point can be determined. In Figure 2, the value of f_w for $R = 0$ is given by a cross for the no flue case and by a star for $Y = 0.2$. It will be shown later that the major advantage of the separate flue leakage site for wind effect is to allow it to have different wind shelter than the rest of the building.

As with the stack factor, there are differences for the wind effect between the exact numerical solution and the approximating equations. A typical difference in wind factors was found to be about ± 0.005 , or with f_w typically 0.2, an error of $\pm 2.5\%$. Thus, the maximum error in f_w is about ± 0.02 or about $\pm 10\%$.

Houses With Crawl Spaces

For a house with a crawl space, the pressure inside the crawl space was approximated in AIM-2 by the average of the four walls, which changed the dependence of f_w on X and R . Using this assumption changed both the exact numerical solution (see Appendix) and the required approximating function. Therefore a different wind factor was required for houses with crawl

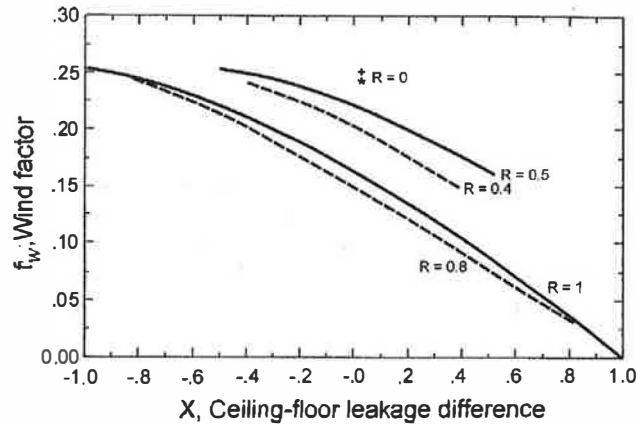


Figure 2. AIM-2 [Equation (18)] wind factor f_w with no flue leakage ($Y=0$) (solid line) and with 20% of leakage in flue ($Y = 0.2$), and $Z_f = 1.5$ (dashed line)

spaces f_{wc} . The algebraic approximation for f_{wc} was developed using the same methods as f_s and f_w and is given by:

$$f_{wc} = 0.19(2-n)X^*R^*Y^* \quad (20)$$

where

$$R^* = 1 - R\left(\frac{n}{2} + 0.2\right) \quad (21)$$

$$Y^* = 1 - \frac{Y}{4} \quad (22)$$

$$X^* = 1 - \left[\left(\frac{X - X_s}{2 - R} \right)^2 \right]^{\frac{3}{4}} \quad (23)$$

and
$$X_s = \frac{1-R}{5} - 1.5Y \quad (24)$$

The critical value of the floor-ceiling difference fraction X_{crit} , above which f_{wc} does not change with X is given by

$$X_{crit} = 1 - 2Y \quad (25)$$

In the AIM-2 approximation, if $X > X_{crit}$ then X is set equal to X_{crit} .

For the case where all the leaks are in the walls ($R = 0$) the wind factor for houses with crawl spaces should be the same as houses without crawl spaces. Using Equation (21) for this case is $f_{wc} = 0.276$, which is 3% less than for a house with no crawl space. The small difference represents the error caused by using approximating functions for f_w and f_{wb} .

Three other wind tunnel data sets, ASHRAE (1989), Liddament (1986), and Wiren (1984), for wall and roof pressure coefficients were also used to find numerical solutions for f_w . These other sets of pressure coefficients produce wind factors that are functionally the same, but that have a difference in the magnitude of the leading coefficient 0.19 in Equations (16) and (18). The two extreme results were taken from Wiren's and ASHRAE's data sets. These produce values of f_w that are respectively 10 to 20% larger and 10 to 20% smaller compared to the values of f_w found using the data set from Akins et al.

The exact numerical flow balance equations were used to estimate the variability of f_w with wind direction. These exact calculations of the ventilation rate for each wind direction using pressure coefficients from Akins et al. introduced a variability in f_w of about $\pm 10\%$ with wind direction. The AIM-2 model neglects these wind direction effects.

Combining Wind and Stack Effect Flows

The superposition technique used in AIM-2 adds the stack and wind driven flows non-linearly, as if their pressure differences added. It also introduces an extra term to account for the interaction of the wind and stack effects in producing the internal pressure that acts to balance the flows in and out of the building. The AIM-2 model uses a simple, first-order, neutral pressure-level shift that produces the superposition:

$$Q = \left(Q_s^n + Q_w^n + B_1 (Q_s Q_w)^{\frac{1}{2n}} \right)^n \quad (26)$$

where Q is the total flow due to combined wind and stack effects (m^3/s), and B_1 is the stack and wind effect interaction coefficient, assumed constant. A study of superposition effects in air infiltration models was performed by Walker and Wilson (1993) to show that simple pressure addition superposition with $B_1 = 0$ can produce as little bias as the superposition technique used here. However, further parametric studies have shown that the interaction term with $B_1 \neq 0$ is necessary when applied over a wider range of leakage distributions.

The constant B_1 was determined empirically using direct measurements of air infiltration. Analysis of data from the six test houses in several different leakage configurations for periods where Q_s and Q_w were approximately equal, suggested that a reasonable estimate for B_1 is -0.33 . As discussed further in Walker and Wilson (1993), this analytical method involved least squares fitting to data at low temperature differences to determine the relationship between wind-speed and measured ventilation rate, and similarly, using low windspeed data to determine an empirical relationship between the temperature difference and the measured ventilation rate. These empirical relationships were then used to calculate Q_s and Q_w for any wind speed or temperature difference. Equation (26) was then used to estimate the total ventilation rate and compare it to the measured ventilation rate for different values of B_1 . The value of B_1 used here proved to be the most appropriate over a wide range of leakage distributions. However, different values of B_1 would give better results for some specific leakage distributions, so this value of B_1 is not universal, it just represents the best compromise for the widest range of conditions. Fortunately, the agreement between measured and predicted ventilation rates was not very sensitive to the value of B_1 because it is a second order effect (compared to the sensitivity to f_s and f_w , for example). Given the scatter in measured data, selection of other values for B_1 did not make much difference to the comparison of measured and predicted values. Because B_1 is negative it reduces the total infiltration rate from the level predicted by a simple sum of pressure superposition.

It is important to keep in mind that the interaction coefficient B_1 is the only constant that was determined empirically from the measured infiltration data. Model evaluation, described in the

following section used data sets chosen to be dominated by wind or stack effects, so that interaction term in Equation (24) involving the empirical coefficient B_1 was negligible. In this way, the model could be tested against independent infiltration measurements that played no part in its development.

Comparison of AIM-2 With Other Ventilation Models

The other models included for comparison to AIM-2 and measured data were: the LBL (USA) model (Sherman and Grimsrud 1980), the VFE (Canada), the variable n extensions of the LBL model by Yuill (1985) and by Reardon (1989), the NRC (Canada) model of Shaw (1985), and the BRE (U.K.) model of Warren and Webb (1980).

The two models that most closely resemble AIM-2 use variable leakage distribution. They are orifice flow model from Sherman and Grimsrud (1980) (often referred to as the LBL model), and a variable flow exponent model, adapted by Reardon (1989) from Yuill's (1985) extension of Sherman's model that used a power law for envelope leakage. The significant differences between AIM-2 and Sherman's and Yuill's models are:

- AIM-2 does not assume a zero pressure coefficient for the attic or floor level leaks.
- AIM-2 differentiates between houses with crawl spaces and those with basements or slab-on-grade construction.
- In AIM-2 the furnace flue is incorporated as a separate leakage site, at a normalized height Z_f above the floor.
- AIM-2 uses a power law pressure-flow relationship.
- AIM-2 includes a wind-stack pressure interaction term that accounts empirically for the building internal pressure.

The two other ventilation models included in this paper for comparison do not allow for variable leakage distribution. A model developed in the U.K. by Warren and Webb (1980) gave three different stack and wind factors, based on the building configuration: detached, semi-detached, and terraced (row houses). The model developed by Shaw (1985) calculated stack and wind flow rates using coefficients fitted to measured data at a single test house.

Evaluation of Models with Measured Air Infiltration

AIM-2 and the other models were evaluated by comparing predictions to air infiltration measurements in two houses at the Alberta Home Heating Research Facility. Continuous hourly infiltration measurements were carried out in the test houses using a constant concentration SF_6 tracer gas injection system in each house described in detail by Wilson and Dale (1985) and Wilson and Walker (1992). The test houses were single-story, wood frame construction with full poured concrete basements; they were numbered four and five at the test facility. An important aspect of the test facility is that the houses were situated in rural terrain. Because the houses were in an east-west row they were unsheltered for winds from the North and South and provided strong shelter for each other for east and west winds.

Envelope leakage characteristics were measured in the two houses using a fan pressurization test over the range from 1 Pa to 75 Pa, from which C, n , and the 4 Pa leakage area A_4 were determined (see Table 2). To remove the effect of building size on the predictions the ventilation rates were converted from m^3/s to air changes per hour (ACH) by dividing by the building volume (approximately 220 m^3 for the test houses in this study).

The leakage distribution was estimated by visual inspection at the test facility. For House #4 with the flue blocked it was estimated that $R = 0.5, X = 0, Y = 0$. For House #4 with a 75 mm diameter orifice in a 150 mm diameter flue it was estimated that $R = 0.3, X = 0, Y = 0.4$. For

Table 2. House Leakage Characteristics

House Number	Flue Configuration	Flow Coefficient, C , $\text{m}^3/(\text{s}\cdot\text{Pa}^n)$	Flow Exponent, n	Leakage Area at 4 Pa (A_4), cm^2
4	Closed	0.007	0.70	65
4	Open with 75 mm diameter orifice	0.010	0.66	93
5	Open with 150 mm diameter flue	0.020	0.58	158

House #5 with a 150 mm diameter flue $R = 0.1$, $X = 0$, $Y = 0.6$. Later, the variability in R and X produced by having different people make these estimates will be discussed.

The models were compared by testing their ability to predict wind and stack dominated ventilation rates separately. The effects of different superposition methods for combining wind and stack effect were discussed elsewhere by Walker and Wilson (1993). The ability of the models to predict average hourly ventilation rates for given ambient weather conditions is shown by their bias and scatter compared to the measured data.

The measured data was sorted into bins covering 5°C indoor to outdoor temperature difference for stack dominated ventilation and 1 m/s wind speed ranges for wind dominated ventilation. The criteria for wind dominated ventilation were $U > 1.5$ m/s and $\Delta T < 10^\circ\text{C}$. For stack dominated ventilation the criteria were $U < 1.5$ m/s and $\Delta T > 10^\circ\text{C}$. To be able to sort for high and low wind speeds and temperature differences, and still provide enough data for binning, a large number of hours of ventilation monitoring were required. For this study 2201 hours were measured in House #4, and 1254 in House #5. Large quantities of data were required due to the substantial hourly variation in ventilation rates.

The average weather conditions for each bin were used as the input values to the models and the model predictions for a given bin were compared to the average measured ventilation rate in the bin. Bias indicates the average error that would be obtained over a long time period if each bin of wind speed or temperature difference were equally likely to occur. Scatter is the variation between the predicted and measured averages from bin to bin, and is an indicator of how well the models follow trends in the data if the bias is removed. The bias can be thought of as the error in proportionality constants, and the scatter as the error in the functional form of the models.

The predictions of AIM-2 and the other four models were compared to measured data in Table 3 for unsheltered conditions (north and south winds) for House #5 with a 150 mm diameter flue, and for House #4 with the flue blocked. These results show that AIM-2 has the best overall performance for houses both with and without furnace flues. For houses with a flue, AIM-2 is clearly superior because the furnace flue is treated as a separate leakage site with its own wind pressure and wind shelter coefficients. For the VFE and LBL models the furnace flue leakage is assumed to be in the ceiling. The other two models do not separate the leakage by location on the building envelope so that the flue leakage is simply included in the total leakage for the building, and not concentrated at a single location. The same data used to calculate bias and scatter in Table 3 are shown in Figures 3 and 4 with binned data where the mean is shown by a square symbol and one standard deviation by error bars.

Figure 6 compares the windspeed dependence of the models for House #5 with an open 150 mm diameter flue where the house is heavily sheltered (east and west winds). All the models except AIM-2 significantly under-predict the wind effect infiltration rate Q_w because they cannot have an unsheltered flue outlet with a sheltered building.

The same data points that were binned for Figure 6 are shown individually in Figure 5. This shows the amount of variation present in the measured data and the need for data binning for model comparisons. The measured variation was mainly due to the wind speed and direction variability during the one hour averaging period for the measured data where one standard devi-

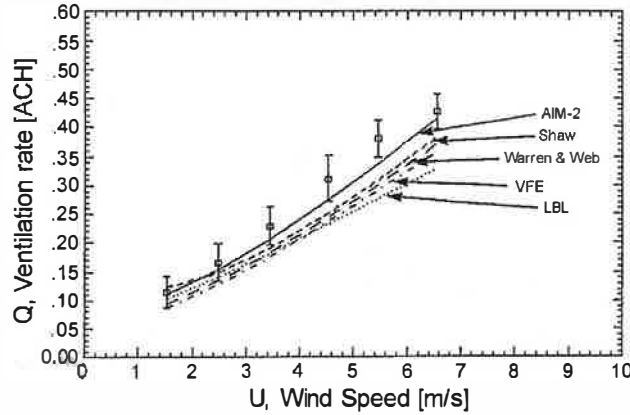


Figure 3. Comparison of ventilation models with measured data for unshielded windspeed dependence (north and south winds) in House #5 (with open, 150 mm diameter flue, $\Delta T < 10$ K, and $U > 1.5$ m/s for 279 hours)

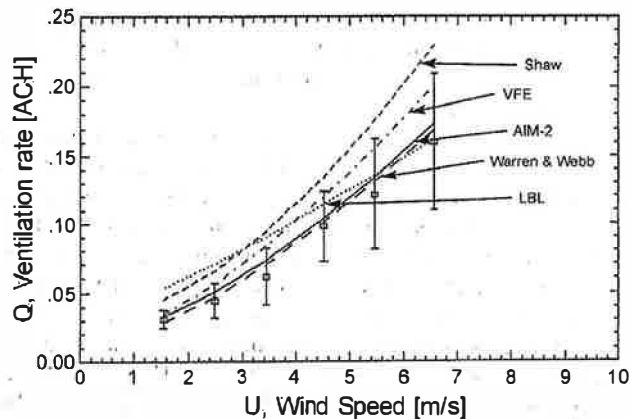


Figure 4. Comparison of ventilation models with measured data for unshielded windspeed dependence (north and south winds) in House #4 (with no flue, $\Delta T < 10$ K, and $U > 1.5$ m/s for 285 hours)

ation for a single bin (a range of wind speeds of 1 m/s) is about 0.04 ACH. The uncertainty of the infiltration measurements themselves was about $\pm 5\%$ or ± 0.004 ACH (from Wilson and Dale 1985). Table 4 presents a summary of the bias and scatter for each model for wind dominated sheltered buildings, along with model predictions for a house without a flue. The models of Shaw, Warren, and Webb over-predict in part because they are incapable of accounting for the variation in leakage distribution.

Figure 7 illustrates the temperature difference dependence of the models for House #4 with a 75 mm diameter restriction orifice in the flue, and Table 5 presents a summary of the bias and scatter for stack dominated ventilation. AIM-2 gave the best overall agreement because it allowed the flue leakage to be above the ceiling height for stack effect. Table 5 also includes the model errors for stack dominated ventilation in House #5 with no flue. As with wind dominated ventilation, the assumptions about leakage distribution and model coefficients from limited data

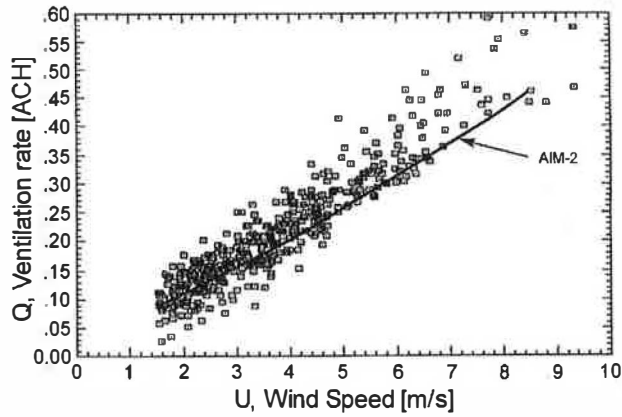


Figure 5. Comparison of AIM-2 with unbinned measured data for shielded windspeed dependence (east and west winds) in House #5 (with open 150 mm diameter flue, $\Delta T < 10$ K, $U > 1.5$ m/s, and 461 hours of unbinned data)

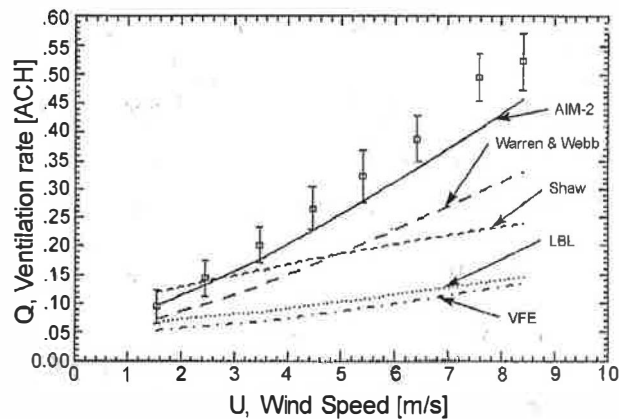


Figure 6. Comparison of ventilation models with measured data for shielded windspeed dependence (east and west winds) in House #5 (with open 150 mm diameter flue, $\Delta T < 10$ K, and $U > 1.5$ m/s for 461 hours)

sets introduced large errors into the model predictions of Shaw and Warren and Webb. In most cases the LBL model had the greatest scatter. This was because its assumption of orifice flow for the building envelope produces an incorrect variation in ventilation rate with wind speed and temperature difference.

Sensitivity to Leakage Distribution

One of the most difficult input parameters to estimate is the distribution of leakage between the floor, walls and ceiling. To estimate the magnitude of variation likely to occur in ventilation rates predicted using different leakage distributions, an informal survey of the staff working at Alberta Home Heating Research Facility was conducted. The survey resulted in eight different estimates of leakage distribution for House #4.

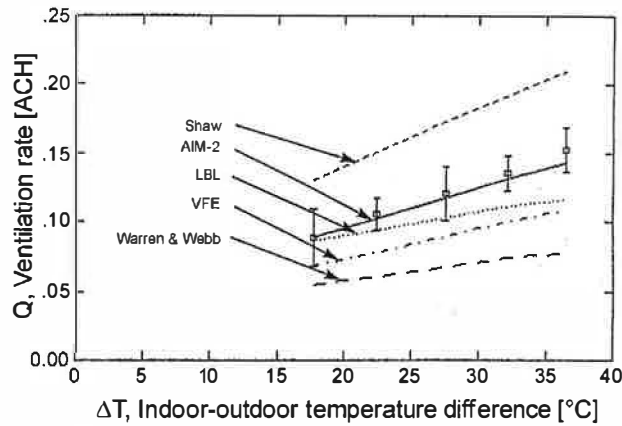


Figure 7. Comparison of ventilation models to measured data for temperature difference dependence in House #4 (with open 75 mm diameter orifice in flue, $\Delta T > 10$ K, $U < 1.5$ m/s, $R = 0.3$, $X = 0$, $Y = 0.4$, and $Z_f = 1.5$ for 102 hours)

Table 3. Differences Between Model Predictions and Measured Data for Binned Averages on Wind Dominated Ventilation for Unsheltered Buildings at AHHRF

Model	House 4: No Flue (285 hours)		House 5: 150 mm Flue (279 hours)	
	Bias	Scatter	Bias	Scatter
AIM-2	10% (0.008 ACH)	3% (0.002 ACH)	-8% (-0.022 ACH)	4% (0.011 ACH)
LBL (Sherman)	34% (0.018 ACH)	18% (0.016 ACH)	-20% (-0.061 ACH)	6% (0.016 ACH)
VFE (Yuill/Reardon)	25% (0.022 ACH)	4% (0.003 ACH)	-22% (-0.059 ACH)	3% (0.009 ACH)
Shaw	45% (0.038 ACH)	2% (0.002 ACH)	-12% (-0.038 ACH)	8% (0.017 ACH)
Warren and Webb	4% (0.005 ACH)	5% (0.003 ACH)	-19% (-0.051 ACH)	2% (0.009 ACH)

The estimated leakage distributions covered a range of 10% to 45% for floors, 35% to 60% for walls, and 20% to 40% for the ceiling. These were significant changes in leakage distribution and indicated the uncertainty with which these values may be estimated, even by people familiar with the structure in question. This range of leakage distribution parameters resulted in predicted ventilation rates from 0.91 to 0.105 ACH, or about $\pm 7\%$ of the average. However, due to the nonlinear nature of ventilation flows this relatively small uncertainty occurs only if the leakage distribution is varied over a reasonable range. Putting all of the leakage in a single location can cause large changes in calculated ventilation rate. e.g. putting all of the leakage in the ceiling would result in zero ventilation because all of the leakage would experience the same pressure difference.

Errors due to leakage distribution estimates were reduced for houses with furnace and fire-place flues because a significant proportion of the leakage has a specific, well known, size and location. This analysis showed that estimates of leakage distribution are not critical unless extreme values are used.

Table 4. Model Errors for Binned Averages of Wind Dominated Ventilation for a Sheltered Building at AHHRF

Model	House 4: No Flue (464 hours)		House 5: 150 mm Flue (461 hours)	
	Bias	Scatter	Bias	Scatter
AIM-2	2% (0.003 ACH)	14% (0.006 ACH)	-12% (-0.041 ACH)	4% (0.011 ACH)
LBL (Sherman)	11% (0.002 ACH)	14% (0.008 ACH)	-60% (-0.199 ACH)	28% (0.078 ACH)
VFE (Yuill/Reardon)	-27% (-0.014 ACH)	7% (0.004 ACH)	-66% (-0.215 ACH)	23% (0.063 ACH)
Shaw	65% (0.030 ACH)	13% (0.007 ACH)	-29% (-0.122 ACH)	30% (0.084 ACH)
Warren and Webb	43% (0.027 ACH)	24% (0.011 ACH)	-35% (-0.112 ACH)	6% (0.014 ACH)

Table 5. Model Errors for Binned Averages of Stack Dominated Ventilation

Model	House 4: 75 mm Flue (102 hours)		House 5: No Flue (74 hours)	
	Bias	Scatter	Bias	Scatter
AIM-2	-3% (-0.005 ACH)	2% (0.002 ACH)	1% (0.001 ACH)	7% (0.005 ACH)
LBL (Sherman)	-14% (-0.019 ACH)	7% (0.008 ACH)	24% (0.015 ACH)	12% (0.009 ACH)
VFE (Yuill/Reardon)	-26% (-0.032 ACH)	2% (0.002 ACH)	4% (0.002 ACH)	7% (0.005 ACH)
Shaw	42.6% (0.051 ACH)	2% (0.002 ACH)	45% (0.032 ACH)	7% (0.005 ACH)
Warren and Webb	-44% (-0.054 ACH)	5% (0.006 ACH)	-22% (-0.018 ACH)	9% (0.007 ACH)

CONCLUSIONS

A simple algebraic model, AIM-2, was developed to calculate ventilation rates from weather conditions and building leakage parameters. The explicit relationships in AIM-2 were developed to reproduce the results of numerical solutions of the exact flow balance equations. Over 3400 hours of measured ventilation rates were used to validate the AIM-2 predictions. By comparing the performance of AIM-2 to both measured data and other simple ventilation models the following conclusions can be made:

- The power law flow relationship and the separate treatment of the furnace flue were significant improvements, reducing errors by up to a factor of five.
- Including the furnace flue (or fireplace) as a separate leakage site allows AIM-2 to account for the effect of the flue on natural ventilation rates better than the other simple models tested in the paper. This is because the furnace flue is located at a different height for stack effect and has its own wind pressure coefficient and wind shelter factor.
- Using a power law pressure-flow relationship ensures that AIM-2 has the appropriate functional form for the dependence of ventilation rate on the wind and stack pressures.
- Typical differences between measured ventilation rates and AIM-2 model predictions were about $\pm 10\%$

APPENDIX: EXACT NUMERICAL SOLUTION TO FLOW EQUATIONS

AIM-2 and this numerical solution use the same method of separating leak location and generating stack and wind effect pressures. The numerical ventilation model explicitly states the flow through each leak location as a function of the amount of leakage at that location and the effective wind and stack pressures acting at that location. The effective pressure across the leak includes the change in interior pressure of the building required to balance the flows in and out through the envelope. The change in interior pressure is common to the flows for all the leaks and is determined numerically so that the inflow through the envelope is equal to the outflow. Once this internal pressure is known, then the flows through all the leaks and the total ventilation flow are also known. Combining this total flow with the total envelope leakage and the wind and stack effect pressures allows the calculation of wind and stack factors (f_w and f_s) determined from an exact numerical solution.

Stack Effect

The following example calculation shows how the exact equations were developed. In this case, $T_{in} > T_{out}$ and the neutral pressure plane lies below the ceiling. The same approach was used for other cases, but not given here, for brevity. The height of each leak was given in non-dimensionalized form (Z). It was non-dimensionalized by dividing by the height of the ceiling above grade. At the neutral pressure plane: $Z = Z_o$. Ceiling leaks have outflow.

$$Q_{ceiling} = C_c \Delta P_s^n (1 - Z_o)^n \tag{A1}$$

Floor leaks have inflow.

$$Q_{floor} = C_f \Delta P_s^n (Z_o)^n \tag{A2}$$

The furnace/fireplace flue(s) have outflow.

$$Q_{flue} = C_{flue} \Delta P_s^n (Z_f - Z_o)^n \tag{A3}$$

The walls have inflow below the neutral level and outflow above it. Also, the flow generated by the pressure difference profile must be integrated over the wall due to the non-linearity of flow with pressure. For this integration, an element of the wall was determined by its fraction of the total wall height and is given by:

$$dC_w = \frac{C_w dZ}{H} \tag{A4}$$

This fractional wall height was expressed in nondimensional height

$$dZ = dz/H \tag{A5}$$

Assuming that the leaks are evenly distributed with height over the wall, then the incremental flow dQ_w to be integrated becomes

$$dQ_{wall} = C_w [\Delta P_s (Z_o - Z)]^n dZ \tag{A6}$$

Below the neutral level the infiltration flow is

$$Q_{wallin} = C_w \Delta P_s \int_0^{Z_o} (Z_o - Z)^n dZ \quad (A7)$$

Performing the integration gives

$$Q_{wallin} = C_w \Delta P_s^n \frac{Z_o^{n+1}}{n+1} \quad (A8)$$

Similarly, for flow out above the neutral level

$$Q_{wallout} = C_w \Delta P_s^n \frac{(1 - Z_o)^{n+1}}{n+1} \quad (A9)$$

Equations (A1), (A2), (A3), (A8) and (A9) can be written in terms of R , X , and Y , and all the inflow terms grouped together to give

$$Q_{stackin} = C \Delta P_s^n \left[\frac{(R-X)}{2} Z_o^n + \frac{(1-R-Y)}{n+1} Z_o^{n+1} \right] \quad (A10)$$

Similarly for the outflows

$$Q_{stackout} = C \Delta P_s^n \left[\frac{(R+X)}{2} (1 - Z_o)^n + \frac{(1-R-Y)}{n+1} (1 - Z_o)^{n+1} + Y(Z_f - Z_o)^n \right] \quad (A11)$$

Setting the inflows and outflows equal gives a single equation, with a single unknown Z_o

$$X = \frac{R[Z_o - (1 - Z_o)^n] + \frac{2(1-R-Y)}{n+1} [Z_o^{n+1} - (1 - Z_o)^{n+1}] - 2Y(Z_f - Z_o)^n}{Z_o + (1 - Z_o)^n} \quad (A12)$$

Z_o was found using a Newton-Raphson technique.

The net infiltration rate was found by averaging the inflow and outflow together and substituting Equation (A12) for X . After considerable algebraic manipulation, the stack factor was given by

$$f_s = \frac{Z_o^n (1 - Z_o)^n \left(\frac{1 + nR - Y}{n+1} \right) + Y(Z_f - Z_o)^n Z_o^n}{Z_o + (1 - Z_o)^n} \quad (A13)$$

The neutral level determined from the solution to Equation (A12) was substituted in Equation (A13) to obtain a numerical value of the stack factor.

Wind Effect

For wind effect, the pressure across each leak was determined by the pressure coefficient on the exterior surface Cp_i and the interior pressure coefficient Cp_{in} that acts to balance the inflows and outflows. For leak i

$$\Delta P_i = \frac{1}{2} \rho_{out} U^2 (Cp_i - Cp_{in}) \tag{A14}$$

The wind induced flow at each leakage site was then determined by the flow coefficient for each site and the pressure difference calculated using Equation (A14). Setting the inflow and outflow to be equal resulted in a single equation that is solved for the interior pressure coefficient.

Each Cp was taken from measured wind tunnel data. The ceiling Cp and floor Cp were discussed in the main text. The flue pressure coefficient of -0.5 was taken from measured data by Haysom and Swinton (1987) and was corrected for the increased wind speed at the flue top compared to the reference wind speed at eaves height. Using the exponent p from the boundary layer wind profile

$$Cp_{flue} = -0.5 Z_f^{2p} \tag{A15}$$

A value of $p = 0.17$ was used here. Assuming a slab on grade or basement house the flow for the walls and floors is given by Equation (A16).

$$Q_{wall,i} = C \left(1 - \frac{R}{2} + \frac{X}{2} - Y \right) \frac{A_i}{\sum A_i} \left(\frac{1}{2} \rho_{out} U^2 \right)^n (Cp_{wall,i} - Cp_{in})^n \tag{A16}$$

The procedure for a crawlspace is the same except that the floor level leaks were expressed separately. The flow for the ceiling was given by

$$Q_{ceiling,i} = C \left(\frac{R+X}{2} \right) \left(\frac{1}{2} \rho_{out} U^2 \right)^n (Cp_{ceiling} - Cp_{in})^n \tag{A17}$$

and the flow through the flue(s) was

$$Q_{flue} = CY \left(\frac{1}{2} \rho_{out} U^2 \right)^n (-0.5 Z_f^{2p} - Cp_{in})^n \tag{A18}$$

Cp_{in} is then found by grouping the inflows and outflows together (by looking at the sign of the pressure difference across each leak) and equating them. The resulting equation was then solved using a Newton-Raphson numerical technique. The resulting flows were then used to determine the wind factor f_w .

NOMENCLATURE

A_4	effective leakage area for 4.0 Pa pressure difference, m^2	C_c	leakage flow coefficient C of ceiling, $m^3/(s \cdot Pa^n)$ at H
A_i	area of wall i , m^2	C_f	leakage flow coefficient C of floor level leaks, $m^3/(s \cdot Pa^n)$
B_1	wind and stack effect pressure interaction coefficient	C_{flue}	leakage flow coefficient C of flue and fireplaces, $m^3/(s \cdot Pa^n)$ at H_f
C	flow coefficient, $m^3/(s \cdot Pa^n)$	C_w	leakage of walls, $m^3/(s \cdot Pa^n)$

C_p	wind pressure coefficient	Q_{wallin}	inflow through wall, m^3/s
$C_{p_{ceiling}}$	wind pressure coefficient for ceiling leaks	$Q_{wallout}$	outflow through wall, m^3/s
$C_{p_{flue}}$	wind pressure coefficient for flue/fireplace top	R	combined fraction of leakage in the floor plus ceiling
C_{p_i}	wind pressure coefficient for leak i	R^*	crawlspace wind factor parameter for R
$C_{p_{in}}$	wind pressure coefficient for inside building	S_w	total wind shelter factor
$C_{p_{wall,i}}$	wind pressure coefficient for wall i , f_s stack factor	S_{wo}	wind shelter factor for building walls
f_w	wind factor	S_{wflue}	wind shelter factor for flues and fireplaces
f_{wc}	wind factor for a house with a crawlspace	T_{in}	indoor temperature, K
F	flue function	T_{out}	outdoor temperature, K
g	gravitational acceleration, m/s^2	U	wind speed at eaves height at the building site, m/s
H	ceiling height of top story above floor (same as eaves height), m	U_{met}	wind speed at the meteorological site, m/s
H_f	height of flue outlet above floor, m	X	difference in leakage fraction between the floor and ceiling
H_{met}	height at which U_{met} is measured, m	X_c	critical value of X for which neutral level is at ceiling for stack effect
J	wind factor parameter	X_{crit}	critical value of X for which neutral level is at ceiling for wind effect
M	stack factor parameter	X_s	shifted value of X for crawlspace wind factor
n	pressure flow exponent	X^*	crawlspace wind factor parameter for X
p_{met}	power law exponent of wind speed profile at the meteorological station	Y	flue leakage fraction
p	power law exponent of wind speed profile at the building site	Y^*	crawlspace wind factor parameter for Y
Q	flow rate, m^3/s	Z	normalized height above floor
$Q_{ceiling}$	ceiling flow, m^3/s	Z_f	normalized flue height
Q_{floor}	floor flow, m^3/s	Z_o	normalized neutral pressure plane height
Q_{flue}	flue/fireplace flow, m^3/s	δz	area averaged height of terrain roughness elements
Q_s	stack effect flow, m^3/s	ΔP	building envelope pressure difference, Pa
$Q_{stackin}$	stack effect inflow, m^3/s	ΔP_i	pressure across leak i , Pa
$Q_{stackout}$	stack effect outflow, m^3/s	ΔP_s	stack effect reference pressure, Pa
Q_w	wind effect flow, m^3/s	ΔP_w	reference wind pressure, Pa
Q_{wall}	wall flow, m^3/s	ΔT	indoor-outdoor temperature difference, K
$Q_{wall,i}$	wall flow through wall i , m^3/s	ρ_{out}	outdoor air density, kg/m^3

REFERENCES

- Alins, R.E., J.A. Peterka, and J.E. Cermak. 1979. Averaged Pressure Coefficients for Rectangular Buildings. *Wind Engineering* Vol. 1, In Proc. 5th Int. Wind Engineering Conference. pp. 369-380.
- ASHRAE. 1989. Air Flow Around Buildings. Chapter 14, *ASHRAE Handbook—Fundamentals*. Atlanta: ASHRAE.
- ASTM. 1995. Determining Air Leakage by Fan Pressurization. *ASTM Standard E 779-87*. W. Conshohocken, PA: American Society for Testing and Materials.
- Beach, R.K. 1979. Relative Airtightness of New Housing in the Ottawa Area. *Building Research Note No. 149*. Ottawa: National Research Council Canada.
- CGSB. 1986. Determination of Airtightness of Building Envelopes by the Fan Depressurization Method. *CGSB Standard 149.10-M86*. Ottawa: Canadian General Standards Board.
- CHBA. 1994. *HOT2000 Technical Manual*. Ottawa: Canadian Home Builders Association.
- Hamlin, T., and W. Pushka. 1994. Predicted and Measured Air Change Rates in Houses with Predictions of Occupant IAQ Comfort. In Proc. 15th AIVC Conference. Buxton, UK, pp. 771-775.
- Haysom, J.C., and M.C. Swinton. 1987. The Influence of Termination Configuration on the Flow Performance of Flues. Canada Mortgage and Housing Corporation *Research Report*. Ottawa: Mortgage and Housing Corporation.
- Irwin, J.S. 1979. A Theoretical Variation of the Wind Profile Power Law Exponent as a Function of Surface Roughness and Stability. *Atmospheric Environment* (13): 191-194.

- Liddament, M.W. 1986. Air Infiltration Calculation Techniques—An Applications Guide. Bracknell, U.K.: Air Infiltration and Ventilation Center.
- Palmiter, L., and T. Bond. 1994. Modeled and Measured Infiltration II—A Detailed Case Study of Three Homes. Electric Power Research Institute Report TR 102511. Palo Alto, CA: Electric Power Research Institute.
- Palmiter, L., and T. Bond. 1991. Interaction of Mechanical Systems and Natural Infiltration. In Proc. 12th AIVC Conference, Ottawa, Canada, pp. 285-295.
- Palmiter, L., T. Bond, and M. Sherman. 1991. Modeled and Measured Infiltration—A Detailed Case Study of Four Electrically Heated Homes. Electric Power Research Institute Report CU 7327. Palo Alto, CA: Electric Power Research Institute.
- Reardon, J.T. 1989. Air Infiltration Modeling Study. Report #CR5446.3 for Energy Mines and Resources Canada. Ottawa: National Research Council Canada.
- Shaw, C.Y. 1985. Methods for Estimating Air Change Rates and Sizing Mechanical Ventilation Systems for Houses. *Building Research Note* 237. Ottawa: National Research Council Canada.
- Sherman, M.H., and D.T. Grimsrud. 1980. Measurement of Infiltration Using Fan Pressurization and Weather Data. Report #LBL-10852. Berkeley, CA: Lawrence Berkeley Laboratory.
- Sulatisky, M. 1984. Airtightness Tests on 200 New Houses Across Canada: Summary of Results. Buildings Energy Technology Transfer Program Publication No. 84.01. Ottawa: Energy Mines and Resources Canada.
- Walker, I.S. 1989. Single Zone Air Infiltration Modelling. M.Sc. Thesis, Department of Mechanical Engineering, University of Alberta, Edmonton, Canada.
- Walker, I.S., and D.J. Wilson. 1990a. Including Furnace Flue Leakage in a Simple Air Infiltration Model. *Air Infiltration Review* 11(4). Coventry, U.K.: AIVC.
- Walker, I.S., and D.J. Wilson. 1990b. The Alberta Infiltration Model: AIM-2. Technical Report No. 71. Edmonton: University of Alberta, Dept. of Mechanical Engineering.
- Walker, I.S., and D.J. Wilson. 1993. Evaluating Models for Superposition of Wind and Stack Effect in Air Infiltration. *Building and Environment* 28 (2): 201-10. Oxford, U.K: Pergamon Press.
- Walker, I.S., and D.J. Wilson. 1994. Simple Methods for Improving Estimates of Natural Ventilation Rates. In Proc. 15th AIVC Conference, Buxton, UK, September 1994.
- Walker, I.S., T.W. Forest, and D.J. Wilson. 1995. A Simple Model for Calculating Attic Ventilation Rates, Proc. 16th AIVC Conference, Palm Springs, USA.
- Walker, I.S., D.J. Wilson, and M.H. Sherman. 1996. Does the Power Law Rule for Low Pressure Building Envelope Leakage? Proc. 17th AIVC Conference. Goteborg, Sweden.
- Warren, P.R., and B.C. Webb. 1980. The Relationship Between Tracer Gas and Pressurization Techniques in Dwellings. Proc. First Air Infiltration Center Conference, pp. 245-276, Windsor, U.K.
- Wieringa, J. 1980. Representativeness of Wind Observations at Airports. *Bulletin Am. Met. Soc* 61: 962-971.
- Wilson, D.J., and I.S. Walker. 1992. Feasibility of Passive Ventilation by Constant Area Vents to Maintain Indoor Air Quality. Proc. Indoor Air Quality '92. ASHRAE/ACGIH/AIHA Conference.
- Wilson, D.J., and J.D. Dale. 1985. Measurement of Wind Shelter Effects on Air Infiltration. Proceedings of Conference on Thermal Performance of the Exterior Envelopes of Buildings, Clearwater Beach, FL.
- Wilson, D.J., and I.S. Walker. 1991. Wind Shelter Effects for a Row of Houses. Proc. 12th AIVC Conf., Ottawa, Canada.
- Wiren, B.G. 1984. Wind Pressure Distributions and Ventilation Losses for a Single-Family House as Influenced by Surrounding Buildings—A Wind Tunnel Study. Proc. Air Infiltration Centre Wind Pressure Workshop, pp. 75-101, Brussels, Belgium, 1984.
- Yuill, G.K. 1985. Investigation of Sources of Error and Their Effects on the Accuracy of the Minimum Natural Infiltration Procedure. Report for Saskatchewan Research Council. Saskatoon, Canada: Saskatchewan Research Council.

